



## Application of laser-induced breakdown spectroscopy to Arctic sediments in the Chukchi Sea

Dukki Han <sup>a,1</sup>, Young Jin Joe <sup>a,b,1</sup>, Jong-Sik Ryu <sup>c</sup>, Tatsuya Unno <sup>a</sup>, Gibaek Kim <sup>d</sup>, Masanobu Yamamoto <sup>e</sup>, Kihong Park <sup>f</sup>, Hor-Gil Hur <sup>f</sup>, Ji-Hoon Lee <sup>g</sup>, Seung-Il Nam <sup>b,\*</sup>

<sup>a</sup> Jeju National University, Jeju Special Self-Governing Province 63243, Republic of Korea

<sup>b</sup> Korea Polar Research Institute, Incheon 21990, Republic of Korea

<sup>c</sup> Division of Earth and Environmental Sciences, Korea Basic Science Institute, Chungbuk 28119, Republic of Korea

<sup>d</sup> Department of Engine Research, Korea Institute of Machinery and Materials, Daejeon 34103, Republic of Korea

<sup>e</sup> Faculty of Environmental Earth Science, Hokkaido University, Sapporo 060-0810, Japan

<sup>f</sup> School of Earth Sciences and Environmental Engineering, Gwangju Institute of Science and Technology, Gwangju 61005, Republic of Korea

<sup>g</sup> Department of Bioenvironmental Chemistry, Chonbuk National University, Jeonju, Republic of Korea

### ARTICLE INFO

#### Article history:

Received 28 March 2018

Received in revised form 3 May 2018

Accepted 3 May 2018

Available online 16 May 2018

#### Keywords:

LIBS

XRF-core scanning

Western Arctic sediment

Chukchi Sea

Sediment composition

### ABSTRACT

Physical and geochemical investigations coupled with laser-induced breakdown spectroscopy (LIBS) were performed on three surface sediment cores (ARA02B/01A, ARA02B/02, and ARA02B/03A) recovered from the western Arctic Ocean (Chukchi Sea) during the IBRV ARAON 2011 expedition. The LIBS technique was applied to conduct elemental analysis of the Arctic sediments and compare the results to those obtained using an X-ray fluorescence (XRF) core scanner and inductively coupled plasma (ICP) system. The LIBS technique showed an elemental composition similar to that using XRF and ICP in each sediment core. Qualitative and semi-quantitative LIBS analyses provide distinguishable patterns between sediment cores, similar to those observed in the ICP analysis. In particular, the elemental pattern of LIBS responded to the color change of the sediment cores. Dark brown layers in the upper parts of the cores were indicated by the color indices and showed elevated Mn/Al ratios, suggesting the influence of regional variation in terrestrial input since the deglacial period. In this study, grain size distribution and contents of detrital dolomite and organic carbon as well as elemental composition (LIBS) were considered to determine sediment provenance and sedimentation environments during the Holocene. Furthermore, the present study showed that the LIBS technique may be used as an applicable method to unravel regional variations in sedimentary composition in the Arctic Ocean.

© 2018 Elsevier B.V. All rights reserved.

### 1. Introduction

Many common approaches (e.g., electron probe X-ray microanalysis, inductively coupled plasma, laser induced breakdown spectroscopy, scanning electron microscopy-energy dispersive spectrometry, X-ray fluorescence, etc.) are used to determine the presence of elements in materials. Particularly, current laser induced breakdown spectroscopy (LIBS) systems promote simplicity with on-site measurement [1] unlike other techniques that require time-consuming and complicated sample preparation steps as well as expensive equipment and trained operators. Indeed, the LIBS technique that analyzes the spectral emission of a chemical element from laser-induced plasma has been applied to geological survey on Mars. There is growing interest in the technique, largely because of its simple or absent sample preparation as well as a

rapid, less-destructive, and cost-effective screening method for various natural materials ([2] and references cited therein). Similar to other common methodologies, quantitative measurement using LIBS requires standard reference materials, but the certified reference materials are difficult to apply to geological samples (rocks, soils, and sediments) [3]. Although standard-free LIBS approaches using a calibration model or matrix-similar standards has been suggested, it needs considerable developmental effort to be applied to diverse and heterogeneous materials [3]. In application to geological materials, the accuracy of the LIBS technique is influenced by the matrix effect (water content and grain size), but the matrix effect can be minimized by sieving and pelletizing materials [4].

Geochemical investigation based on elemental compositions of marine sediments has been conducted to track climate change at a geological timescale. Indeed, Antarctic marine sediments, analyzed using LIBS, have implied that the LIBS technique may be used to identify sediment provenance in the polar seas [5]. LIBS may be an ideally applicable method for geologists to estimate elemental distribution in marine

\* Corresponding author.

E-mail address: [sinam@kopri.re.kr](mailto:sinam@kopri.re.kr) (S.-I. Nam).

<sup>1</sup> Equal contribution to this study.

sediments, but its applications are limited. Moreover, there is no feasibility study for Arctic marine sediments using the LIBS technique to compare it to traditional approaches such as X-ray fluorescence (XRF) core scanning and inductively coupled plasma (ICP) measurement.

The Arctic Ocean has recently become an important issue due to a rapid reduction in sea-ice extent that globally affects ocean circulation and climate change [6,7]. In particular, the North Pacific inflow from the shallow and narrow Bering Strait (hereafter Bering Strait inflow; BSI) plays an important role in controlling heat, freshwater, and nutrient fluxes to the western Arctic Ocean, and it was highly susceptible to sea-level fluctuations during the late Quaternary ([8,9] and references cited therein). Thus, the BSI signal can provide a means to understand variations in sea-ice and marine production in the western Arctic Ocean [9]. The Bering Strait may have been predominantly closed by the end of the last glacial period (80 000–11 000 years before present) [10]. The lowered sea-level during the last glacial period may have resulted in the limited influx of fresher Pacific Ocean waters into the Arctic Ocean. Although the history of sea level in the Bering Strait has been previously described [11–13], the inflow of Pacific waters during the post glacial period (Holocene) has been poorly estimated because of the lack of high-resolution records. Sediment properties have been used to reconstruct paleoclimatic events in the Arctic Ocean ([14,15] and references cited therein). For example, sediment color is generally sensitive to bottom water conditions (such as water depth, Eh, and pH), sediment constituents (such as disseminated organic matter, microbe, and carbonate), and/or diagenesis, texture, and composition of minerals and elements in sediments. In general, mineral and elemental compositions are related to sediment grain size and provenance. Recently, Kobayashi et al. [15] investigated the mineral distribution and color indices of Arctic sediments, and reported that mineral composition is useful for tracking sediment provenance associated with the BSI signal. Moreover, the elemental distribution of Arctic sediments is presumably related to riverine discharge from the hinterland, ice rafted debris (IRD), and ocean circulation in the western Arctic Ocean [14]. In particular, Meinhardt et al. [14] reported that dark brown layers in Arctic surface sediments show an excessive amount of Mn and Fe, and a distinct change in Mn/Al and Fe/Al ratios

seems to reflect a climatically elevated input of Mn and Fe near the sediment/water interface during the late Quaternary interstadial or interglacial periods.

The aim of the present study is to evaluate the feasibility of using the LIBS technique to analyze Arctic sediments. Three surface sediment cores were recovered from the western Arctic Ocean (Chukchi Sea) during the IBRV ARAON 2011 expedition. Physical and geochemical datasets, such as elemental composition (LIBS), grain size distribution, color indices, and organic carbon content, were analyzed for the sediment cores. In particular, the elemental profiles of LIBS were compared to those measured using an ITRAX XRF core scanner and ICP.

## 2. Materials and methods

### 2.1. Field description and sample preparation

Three coring sites from the shelf toward the Chukchi Plateau (ARA02B/01A, ARA02B/02, and ARA03B/03A in Fig. 1a) were selected to obtain sediment cores using a multiple- and box-corer during the IBRV ARAON 2011 expedition (ARA02B). Three box cores were sealed on board for further XRF-core scanning (ITRAX). Every three parallel cores were retrieved from the same multiple-corer at each coring site. A set of the parallel cores was assigned to the present study (here referred to as 01A, 02, and 03A), and the others were kept at the Korea Polar Research Institute (KOPRI) or transferred to Hokkaido University [15]. Cores 01A, 02, and 03A were subsampled at a depth interval of 2 cm and stored in a freezer onboard until undergoing a freeze-drying process. The freeze-dried sediments from the three multiple cores were all used for LIBS, ICP, and grain size analyses, and sediments of the 03A core were additionally analyzed using the Delta V elemental analysis - isotope ratio mass spectrometry (EA-IRMS) at KOPRI.

### 2.2. Sediment analysis

Box cores were split in the laboratory and the split core surfaces were run through an ITRAX core scanner at KOPRI to obtain XRF

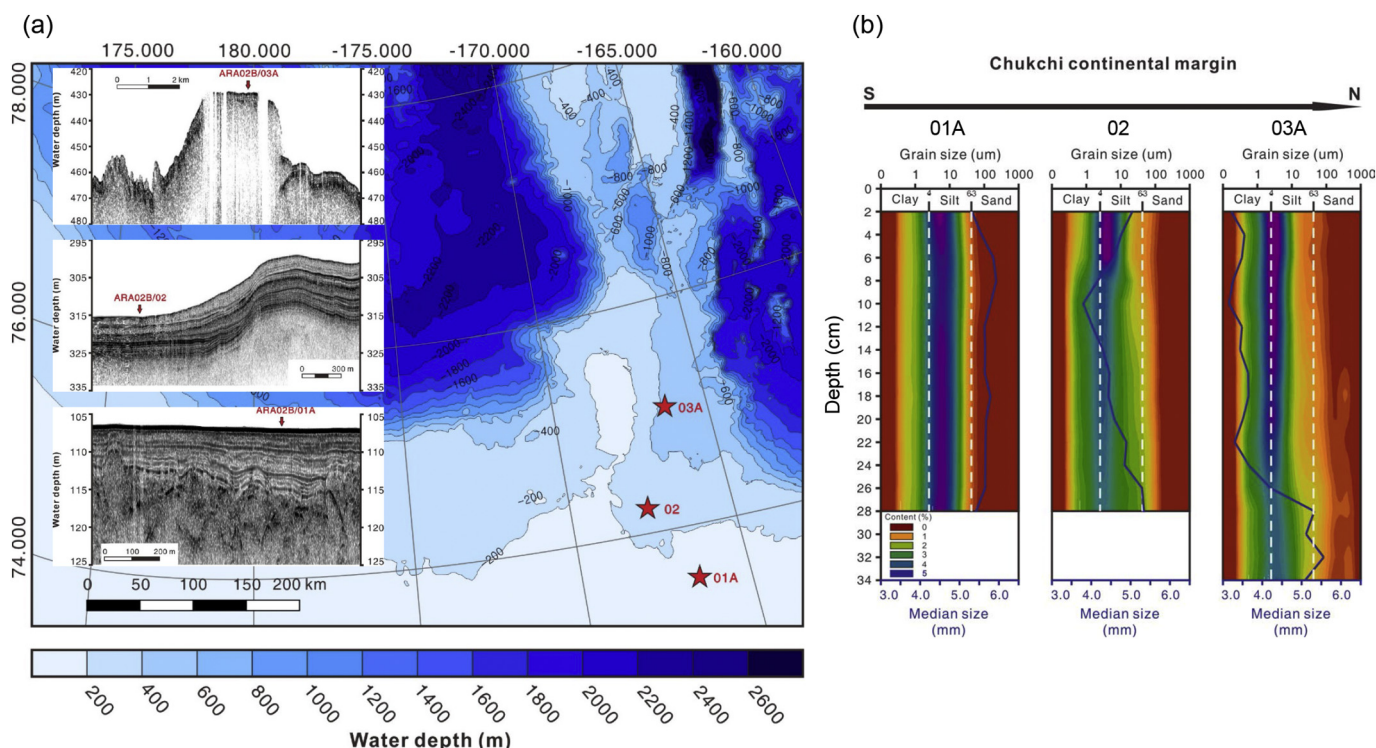


Fig. 1. Description of coring locations with (a) SBP image, and (b) grain size for sediment cores.

measurements of the sediments' elemental composition at a 5-mm depth interval on the basis of a described method [16]. Of the multiple cores, the dried sediment samples were homogeneously ground in an agate mortar. The ground sediments were equally weighed (0.5 g) and then prepared as pressed pellets, with a load of 5000 kg for 1 min. Pellet samples were immediately analyzed using LIBS according to a previously described method [17]. For ICP analysis, approximately 0.1 g of each sample was completely digested in a 5:3 mixture of HF and HNO<sub>3</sub>. The sample was dried, refluxed several times in 6.0 M HCl to remove fluorides, and re-dissolved in 5% HNO<sub>3</sub>. Cation and trace-element concentrations were measured using a Perkin Elmer Optima 4300DU inductively coupled plasma atomic emission spectrometer (ICP-AES) and a Thermo Elemental X-7 inductively coupled plasma mass spectrometer (ICP-MS) at the Korea Basic Science Institute (KBSI). Repeated analyses of U.S. Geological Survey basalt standard powders (BCR-2, BHVO-2, and BIR-1) yielded external reproducibility better than ±5%. For grain-size analysis, approximately 0.3 g of each freeze-dried sediment was treated with 5 mL of 35% H<sub>2</sub>O<sub>2</sub> to decompose organic matter. Then, these samples were rinsed with distilled water three times to remove salt. Grain size measurements in a range of from 0.02 to 2000 μm were made using a Malvern Mastersizer laser particle sizer (Mastersizer 2000) at the Korea Institute of Geoscience and Mineral Resource (KIGAM) that automatically provides the grain composition (e.g., percentage of clay, silt, and sand). The sediment color indices and XRD data originated from a previously published document [15]. Prior to calculating carbonate and organic carbon contents in the sediments, bulk sediments were treated with 10% HCl for 24 h to remove the carbonate. The residues were washed three to five times with deionized water and then dried in an oven at 50 °C. The bulk sediment and carbonate free sediment were measured using a Thermo Flash 2000 CHNS/OH EA connected by means of continuous flow to a Thermo Delta-V EA-IRMS at KOPRI. The carbonate contents were calculated from the following equation [18]. 1) TIC (total inorganic carbon) = TC (total carbon) – TOC (total organic carbon); 2) CaCO<sub>3</sub> = TIC × 8.33 (carbonate/carbon ratio). A geochemistry-based approach [14] was applied using ICP data to estimate the content of biogenic carbonate among the cores. In the present study, data manipulation and analysis were performed using Excel (Microsoft) and R (<http://cran.r-project.org/>).

### 3. Results and discussion

#### 3.1. Sedimentation patterns in the Chukchi Sea during the Holocene

The three multiple cores, collected from different coring sites (O1A: continental shelf; O2: channel slope; and O3A: sea mount) on shallow shelves toward the Chukchi Plateau, showed distinguishable grain size patterns (Fig. 1b). Core O1A consisted mostly of silt-rich sediments (1 to 20 μm) and the vertical grain size distribution was constant throughout the sediment core. Grain composition in core O2 was similar to that of core O1A in the manner in which both cores consisted mostly of fine-grained muds (O1A: ~0.5% sand; O2: 2–6% sand), but the median grain

size was different between each. Core O3A was generally clay-silt, and the sand (>63 μm) content increased below 16 cm below sea floor (hereafter referred to as cm). In the study area, sedimentation patterns at the O1A and O2 coring sites differed from that of O3A. The depositional condition in the Chukchi Sea during the Holocene can be inferred from the downcore grain size distributions in cores O1A, O2, and O3A (Fig. 1b). For example, core O1A shows a constant grain size range from the core top to the bottom, suggesting constant deposition of terrigenous materials under current seasonally ice-covered marine environments. The grain size of core O3A had an obvious boundary layer at 22 cm (coarsening downward), reflecting a distinct change in sedimentation environment probably during the late deglacial period or early Holocene. The occurrence of coarse debris below the 16 cm layer seems to indicate the influence of drifting ice and/or icebergs during the last deglacial phase, implying that the offshore sedimentation environments have gradually changed because of the sea-level rise during the Holocene. Indeed, the O1A coring site presently has deposits under an open marine condition influenced by the BSI [19]. In contrast, the upper horizon (0–20 cm) of O3A consists of clay-rich muddy sediments, and the lower horizon consists of silt with ice-rafted debris (IRD). Thus, the upper brownish layer of core O3A seems to have been deposited during the Holocene, whereas the lower part was deposited during the last warming period.

#### 3.2. Geochemical investigation

##### 3.2.1. Comparison among LIBS, ITRAX, and ICP

In general, an XRF core scanner (herein ITRAX) can provide rapid and undisturbed high-resolution (millimeter-scale) elemental data on the surface of a split sediment core. However, interpretation of the scanning data requires careful consideration because uneven surface roughness of split sediments together with mineral heterogeneities, changes in density and water content/porosity, and grain size at the surface of sediment cores can affect elemental count rates [20]. The present study introduced commonly used elements in marine sediments, instead of describing all analyzed elements using LIBS, ITRAX, and ICP (see raw dataset in the linked electronic repository; [http://biotech. jeju.ac.kr/~mbl/documents/supp.data.xlsx](http://biotech.jeju.ac.kr/~mbl/documents/supp.data.xlsx)). Mg and Si were partially omitted from the elemental dataset due to a technical reason. For example, Si element was not measured by ICP, and ITRAX excluded Mg element under instrument condition although LIBS provided both Mg and Si profiles in the present study. Of the elements, Al, K, Ca, Mn, Fe, and Sr, which were measured together using LIBS, ITRAX, and ICP in cores O1A, O2, and O3A, were compared using non-metric multidimensional scaling (NMDS). In NMDS analysis, the LIBS data were clearly separated into each core compared to that of the ITRAX data (Fig. 2) and rather correspond with the ICP data, suggesting that the LIBS technique can provide more accurate quantitative analysis of elemental content in Arctic sediments. Mg, K, Ca, Mn, Fe, and Sr measured using ICP were also compared to those of LIBS after normalization by Al, which is known to be of terrigenous origin and is less affected from biogenic or diagenetic processes. As shown in Fig. S1, each element/Al in the linear

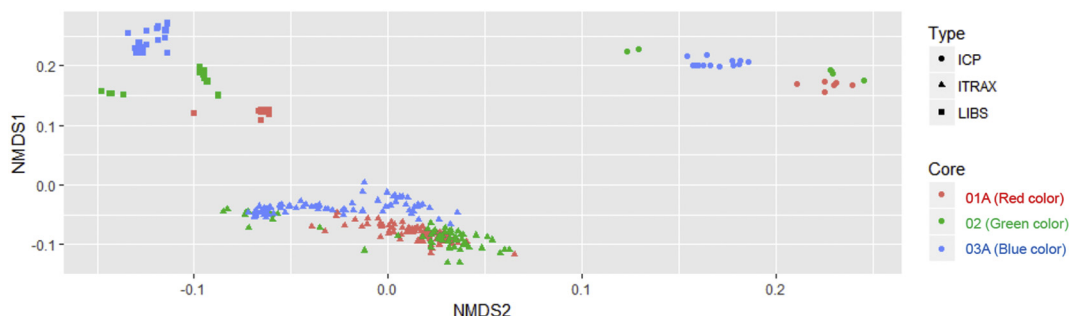


Fig. 2. NMDS analysis for element data set from LIBS, ITRAX, and ICP measurements.

relationships showed varying correlation coefficients in response to each core and element, suggesting that elements require distinctive calibration curves for quantitative LIBS analysis.

Al, Si, K, Ca, Mn, Fe, and Sr contents in cores O1A, O2, and O3A were measured using LIBS, ITRAX, and ICP (Fig. 3). ITRAX and LIBS seem to show a similar pattern in elemental distribution for all cores, although the elemental distribution was estimated using different sediment cores obtained with a multiple- (for LIBS) or box-corer (for ITRAX) at the same coring site. In the case of ICP analysis, there was no wide discrepancy with LIBS and ITRAX except for K and Al in core O3A. Such a discrepancy in core O3A matched the distinct change in grain size at the 22 cm boundary layer, suggesting that the LIBS and ITRAX measurements need to consider sediment grain size.

### 3.2.2. Elemental trends from LIBS measurement

In the LIBS data, all elements were normalized by Al as previously suggested in the Antarctic sediments [5]. Most element/Al ratios except for K/Al showed a distinct shift in their upper part (Fig. 4). All cores showed higher element/Al ratios in the upper part of the core, and their elemental trends seem to be responsive to sediment provenance in the Chukchi margin. In the western Arctic Ocean, Mn enrichment in sediment cores during warm and/or mild interstadial periods resulted from both Siberian river discharge and coastal erosion [14,21]. In particular, a dark brown layer, which the  $L^*a^*b^*$  diagram indicated [15], is relatively well matched with elevated Mn/Al and Fe/Al in the Arctic sediments [14]. Indeed, such a pattern is clearly shown by Mn/Al ratio and color indices (Fig. 5). The color change of core O1A is similar to that of core O2. The upper horizon of core O1A (ca. 2 cm) and O2 (ca. 6 cm) showed lower  $L^*$  (darker) and higher  $a^*$  (more reddish) and  $b^*$  (more yellowish) layers and was assigned a dark brown color. For cores O1A and O2, the dark brown layers correspond well to their Mn/Al profile. In contrast, core O3A shows a distinguishable pattern compared to the other cores. The brown layer of core O3A was assigned to core top 16 cm, below which the Mn/Al ratio clearly decreased. The lower layer below 16 cm would be the dolomite layer as previously indicated [15].

In the western Arctic Ocean, the elevated ratios of Mn/Al or Fe/Al within the uppermost layer of sediment cores represent an enhanced input of Mn and other elements by riverine discharge or erosion of coastal deposits to well oxygenated bottom waters via the continental margin during interglacial/interstadial periods, and, consequently, a dark brownish layer is formed by later diagenetic redistribution ([14] and references cited therein) which can also modify metal concentration patterns [22]. In the present study, the vertical distribution of most elements from LIBS data suggests a close relationship between elemental distribution and sediment provenance toward the Chukchi Plateau. For cores O1A, O2, and O3A, for example, elemental variation characteristics in the uppermost layers were similarly overlapped with grain size patterns, and the dark brown sediments in the uppermost layers were also featured an elevated Mn/Al ratio as shown in Fig. S2.

### 3.2.3. Unit conversion from LIBS to ICP

In general, Al normalization is widely used to minimize the elemental analysis variability in marine sediments [23]. Indeed, element/Al ratios of Fe, Mn, Ca, K, and Sr from LIBS, ITRAX, and ICP showed a parallel trend in core O3A (Fig. S2), although a discrepancy in the elemental profile between LIBS, ITRAX, and ICP occurred below 22 cm in core O3A (Fig. 3). With Al normalization, the trend in the LIBS profile seems to be much more similar to that of ICP (Fig. S2), corroborating the accuracy of LIBS data compared to ITRAX data as shown in the non-metric multi-dimensional scaling (NMDS) pattern (Fig. 2). The present study assumed that LIBS data may be comparable to ICP data, and thus the FORECAST function using a linear regression model in Excel was used to estimate the elemental concentrations (ICP unit) from LIBS values in the cores.

The regression model provides new values for elemental content converted from the pared LIBS data. The converted values were plotted

together and compared to the observed elemental content using ICP, and the comparison between the converted LIBS and the ICP reference values showed a reasonable agreement (Fig. 6). In the elemental profiles, the extrapolated values from the regression model seem to be partially different from ICP references. However, the discrepancy between the converted LIBS values and the ICP reference in the cores occurred in the upper layers (above 10 cm) of core O1A and O2 or the lower layer (below 20 cm) of core O3A. The discrepancy was clearly matched to the distinct change in sediment grain size, implying that irregular grain size possibly results in an overestimated or underestimated conversion from LIBS to ICP.

## 3.3. Feasibility of using LIBS for Arctic sediments

### 3.3.1. The first application of the LIBS technique to Arctic marine sediments

In general, the LIBS technique is known as a less time-consuming and semi-quantitative elemental analysis, and has relatively high levels of sensitivity, precision, and distinction in performance. Moreover, LIBS does not require costly equipment, trained operators, and complicated sample pre-treatment processes. However, there has been no attempt to determine whether the LIBS technique could be used by geologists to understand sedimentary sequences in the Arctic Ocean despite the potentiality of LIBS as an alternative technique. In the present study, qualitative analyses of LIBS and ITRAX have shown similar elemental distribution in Arctic shelf sediments, and the accuracy of LIBS data is also supported by the ICP technique as shown in Fig. S2. In general, XRF data from the ITRAX core scanner is unfavorable for a quantitative measurement as shown in Fig. 2. The LIBS technique has rarely been applied to Arctic sediments, although it is a versatile tool with unlimited applications [24]. The present study found that the LIBS technique can compensate for the defects in quantitative analysis of Arctic sediments. For example, the LIBS peak strength for estimated elements in each core shows a distinguishable pattern in the NMDS analysis. The synchronous elemental pattern from LIBS, ITRAX, and ICP (Fig. S2) supports that the LIBS technique can be useful for elemental analysis of Arctic sediments.

### 3.3.2. Considerable geological features for LIBS accuracy

The present study evaluated the feasibility of using the LIBS technique for Arctic sediments and found that the accuracy of LIBS can be influenced by irregular grain size. It is already known that water content and grain size of geological materials (the matrix effect) can influence the accuracy of the LIBS technique. The sediments in the present study were dried, ground, and pelletized before LIBS measurement to minimize the matrix effect. Perhaps the pelletized sediments still had an uneven surface roughness, which could have affected the spectral emission intensity in the laser-induced plasma. On the other hand, the discrepancy in K and Al between LIBS and ICP in the lower layer of core O3A could be indirectly influenced by the mineral heterogeneity in the IRD layer. The Chukchi Shelf marine sediments in the Arctic Ocean include a high number of silicate minerals, and feldspar ( $\text{KAlSi}_3\text{O}_8 \cdot \text{NaAlSi}_3\text{O}_8 \cdot \text{CaAl}_2\text{Si}_2\text{O}_8$ ) is among the most abundant minerals [15]. Indeed, the lower layer of core O3A consists of sandy muds (5–11% sand) in response to the feldspar-rich IRD layer (Fig. 7), suggesting that the void space between coarse-grained sediments affects the accuracy of LIBS measurement for feldspar-related elements. Perhaps the pelletized sediments sampled from the feldspar-rich IRD layer resulted in a matrix effect bias, and caused overestimation of Na, Al, and K in LIBS measurement as shown in Fig. 7. Thus, geological traits need to be carefully considered for the application of LIBS to Arctic sediments.

### 3.3.3. Further application using LIBS: estimation of biogenic carbonate in Arctic sediments

Geological investigation in the present study evaluated whether specific elemental patterns can track the transport of terrigenous materials. In general, IRD delivered to the Chukchi shelves is recognized as dolomite as indicated by both detrital carbonate and Ca/Al, Zr/Al, Mg,

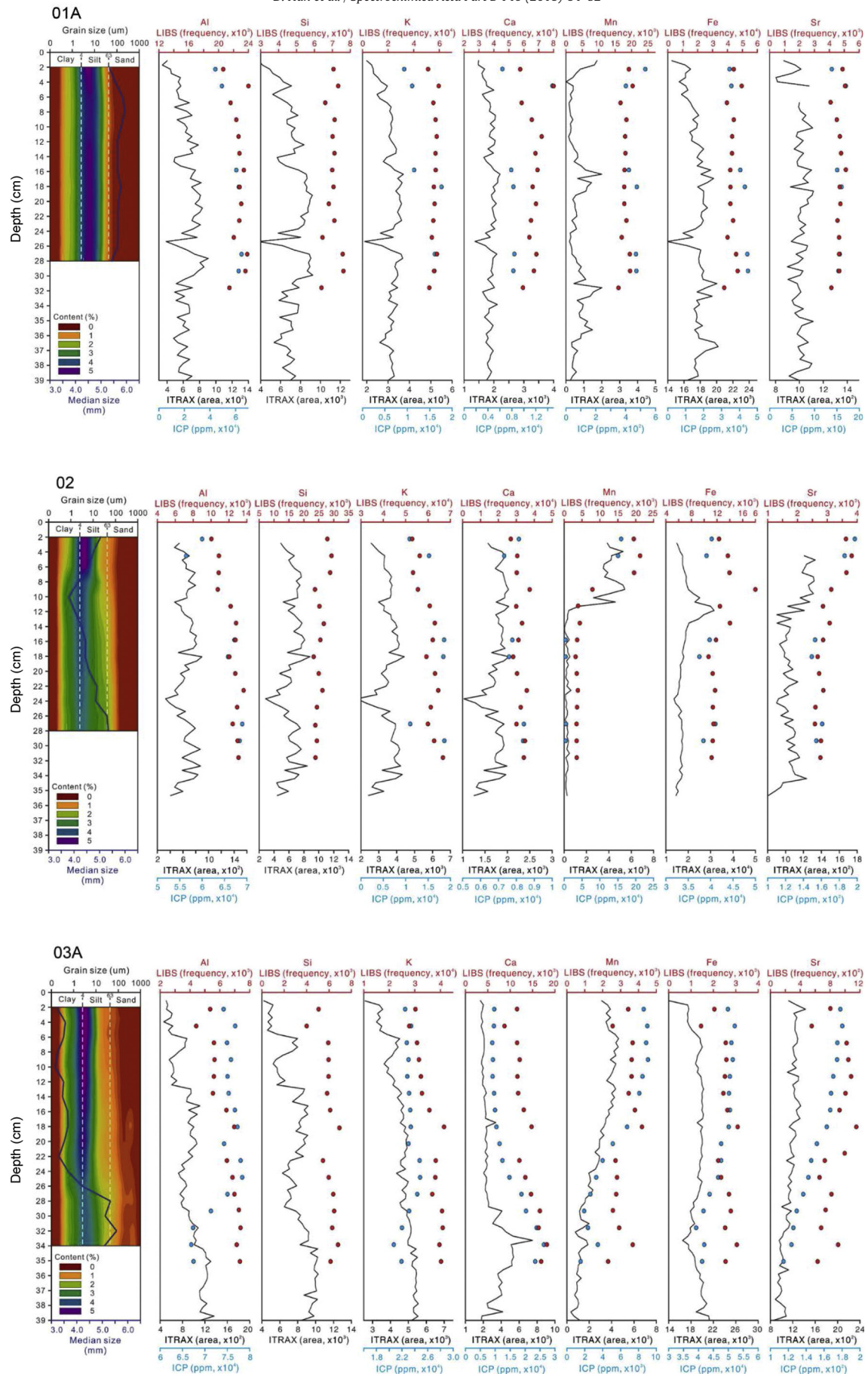


Fig. 3. Comparison between LIBS, ITRAX, and ICP in core O1A, O2, and O3A.

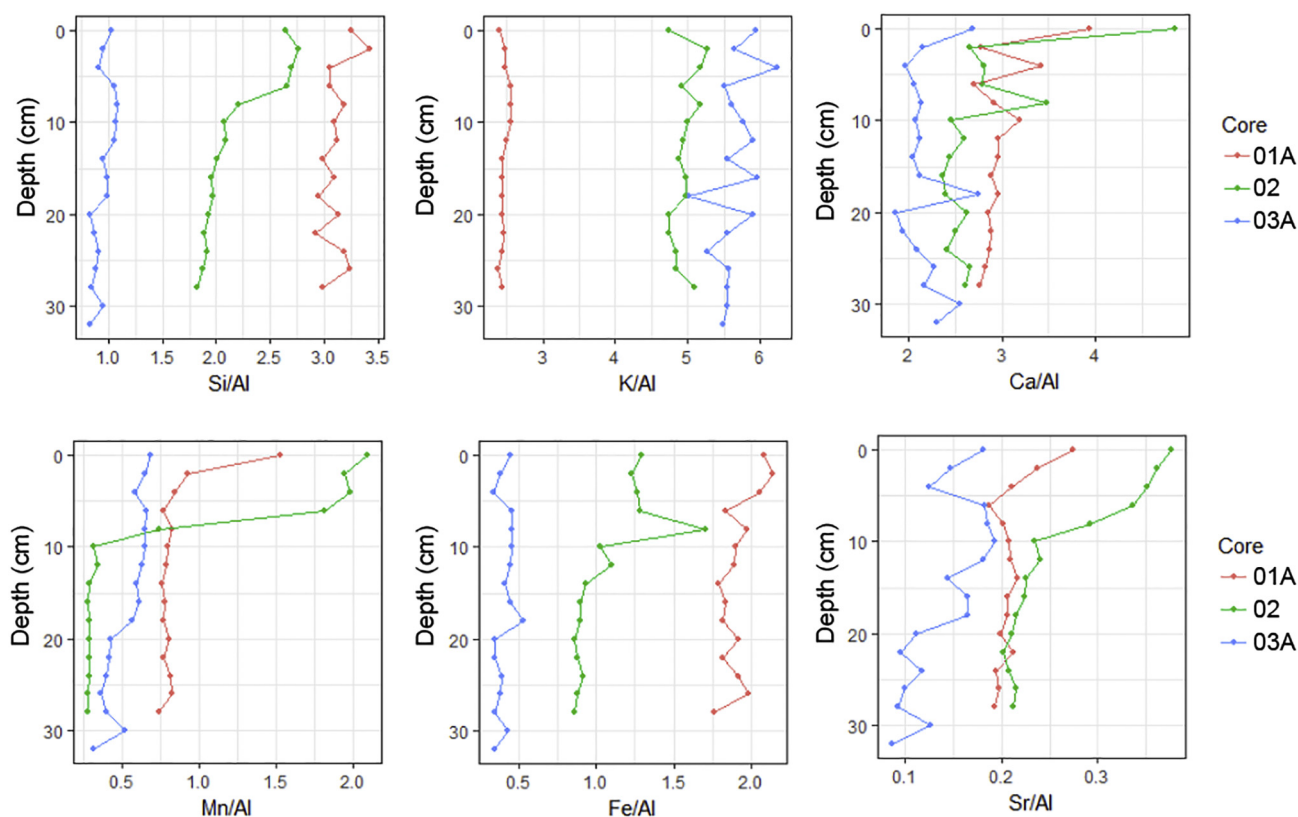


Fig. 4. Element/Al ratio (LIBS) of Mn, Fe, Ca, K, Si, and Sr in core 01A, 02, and 03A.

and TIC [14]. It is well known that detrital carbonate is transported by the Laurentide icebergs from the Canadian Archipelago through Beaufort Gyre toward the western Arctic Ocean [14]. In cores 01A, 02, and 03A, the distribution of Ca and Mg, measured using ICP, seems to be a response to the  $\text{CaCO}_3$  profile calculated from Delta V EA-IRMS data (Fig. S3). In the present study, the elemental content of core 03A was quantitatively measured using ICP with a higher sample frequency than that of cores 01A and 02 to understand the provenance of the dolomite layer as previously indicated in core 03A [15]. In core 03A, Ca and Mg patterns parallel the calculated  $\text{CaCO}_3$  profile, and Ca-rich carbonate occurred at the bottom layer (below 20 cm), indicating the occurrence of dolomite (Fig. 8). Indeed, a dolomite-rich sediment layer was found below 20 cm in parallel with one of three parallel multiple cores at

Hokkaido University (Fig. 8). The fate of the biogenic carbonate in the western Arctic Ocean is complicated by deposition of dolomite due to early degradation of organic carbon in marine sediments during diagenesis. In core 03A, the amount of biogenic carbonate was calculated using a geochemistry-based approach [14], and showed that only limited values of biogenic carbonate paralleled the concurrently increased values of Ca-Mg carbonate in the dolomite-rich sediment layer (Fig. 8).

The present study found that the upper layer sediments (above 20 cm) in core 03A show a similar level of calculated  $\text{CaCO}_3$  contents compared to that of cores 01A and 02 (Fig. S3), whereas increased contents of calculated  $\text{CaCO}_3$  below 20 cm reflect the enhanced terrestrial material input related to the carbonate-bearing IRD derived from the Canadian Arctic archipelago (CAA) via Beaufort Gyre likely during the

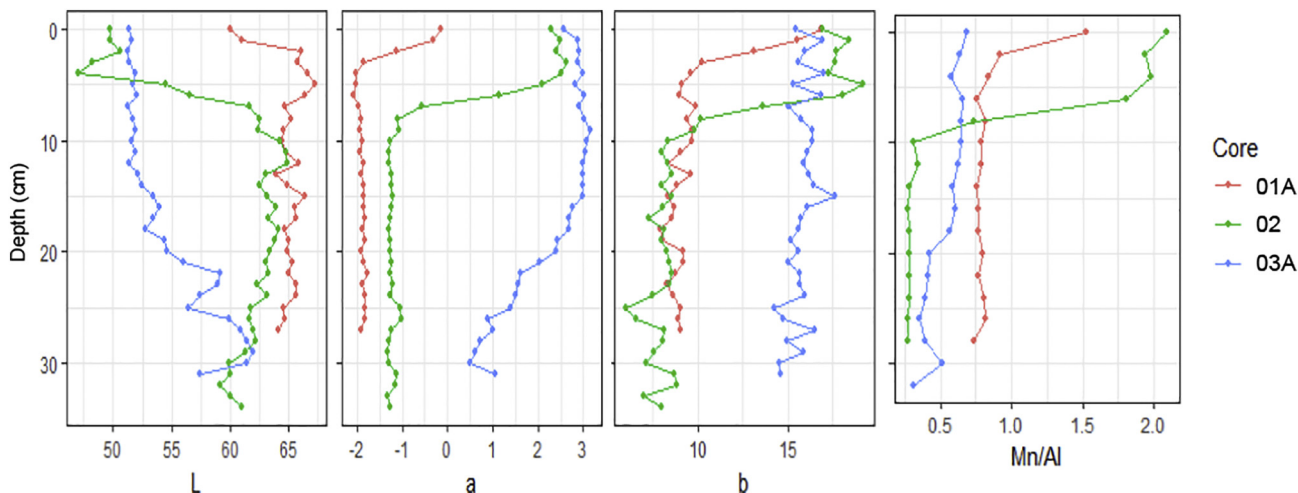


Fig. 5. Comparison of color indexes with Mn/Al ratio (LIBS) in core 01A, 02, and 03A.

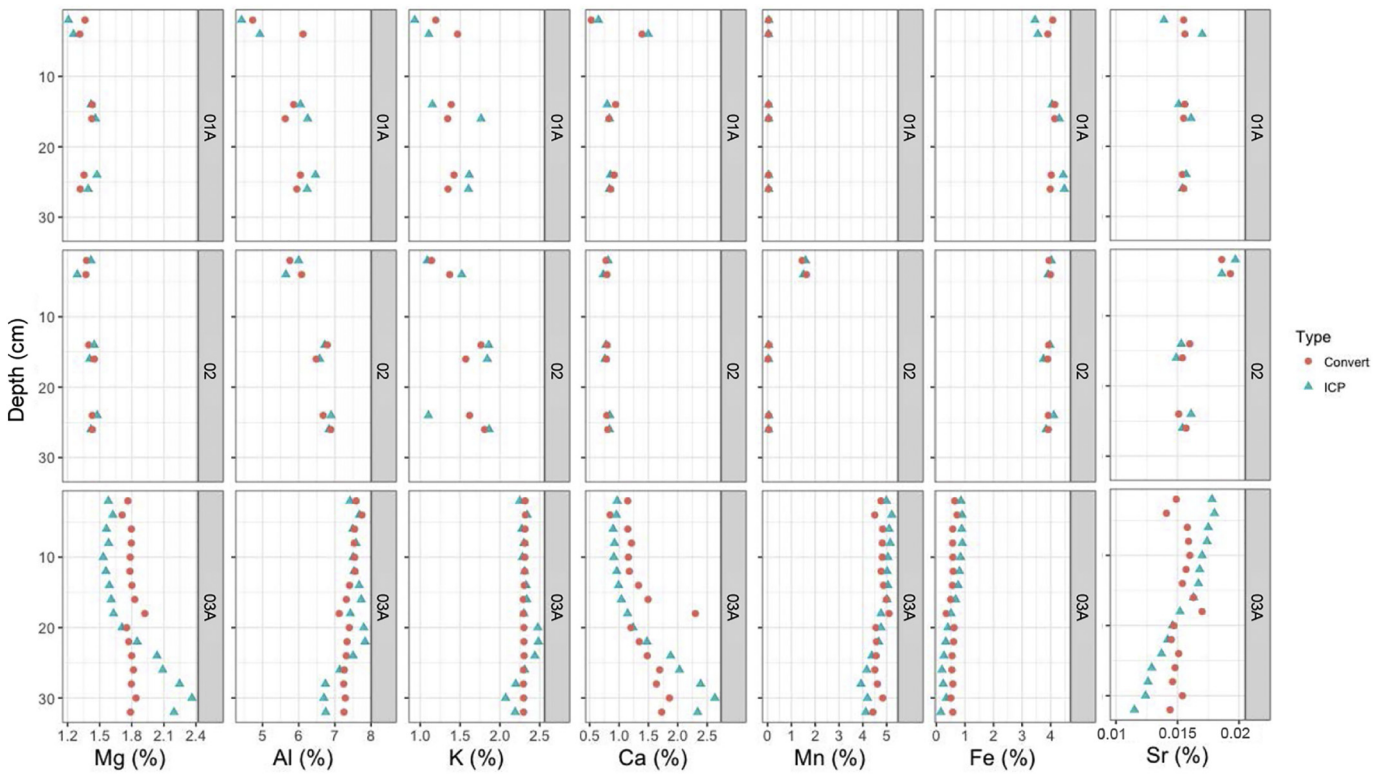


Fig. 6. The converted elemental concentrations from LIBS values using the FORECAST function in Excel in core 01A, 02, and 03A.

last post-deglacial period [6,9,14]. Meinhardt et al. [14] recently estimated the biogenic carbonate contents in Arctic sediments using a geochemistry-based approach. In the present study, the biogenic carbonate seems to be in response to the calculated CaCO<sub>3</sub> profile

(Fig. S3), and is regionally limited in the Chukchi Sea Shelf sediments (01A and 02) or rare on the Chukchi Plateau (03A: 0.11 ± 0.06%) than that found in the deeper offshore sediments of Mendeleev Ridge (by approximately 4%) [14]. In general, the deeper offshore sediments contain

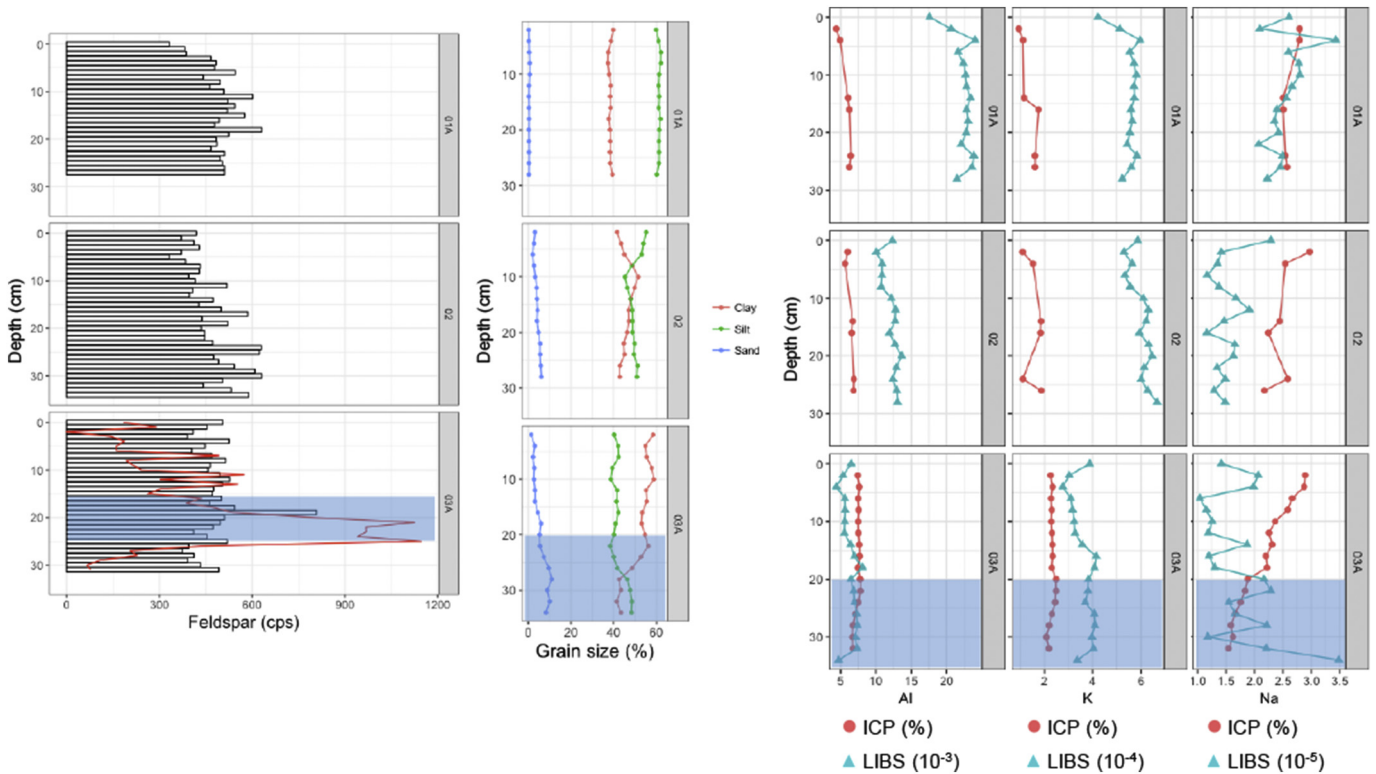
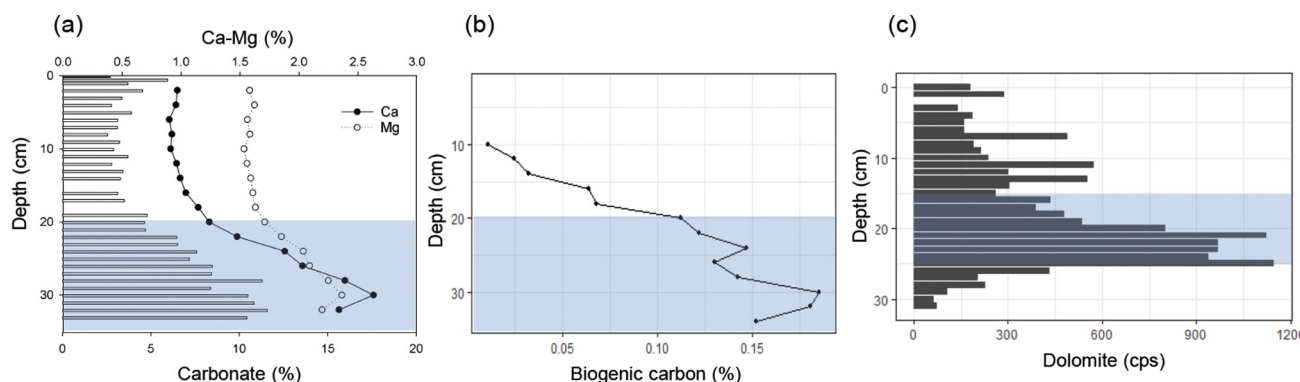


Fig. 7. Distribution of feldspar, gain size, and element Al, K, and Na in core 01A, 02, and 03A.



**Fig. 8.** Distribution of (a) carbonate (calculated from IRMS data) and Ca-Mg (ICP), (b) biogenic carbon (calculated from ICP data), and (c) dolomite (XRD data from Kobayashi et al. [15]) in core 03A. The parallel cores ((a) and (b) from the present study; (c) from Hokkaido Univ.) were comparatively correlated to infer the abiogenic carbonated dolomite layer (blue colored box).

a relatively enhanced abundance of calcareous microfossils such as high contents of foraminifera and low contents of coccoliths and ostracods because of the increase in its productivity during warm intervals. In contrast, Holocene biogenic carbonate contents in the shallow shelf sediments are distinctly lower compared to those in deeper offshore sediments [25], because carbonate contents in shallow continental margins along the western Arctic are dominantly of terrigenous origin mainly transported from the surrounding lands via riverine discharge and coastal erosion. There is very little biogenic carbonate due to suppressed productivity and widespread dissolution in surface sediments [26].

#### 4. Conclusions

The present study illustrates the potentiality of using LIBS for qualitative and quantitative analyses of elemental profiles in Arctic sediments compared to those measured using the ITRAX core scanner. The present study found a limitation in the unit conversion from LIBS to ICP in the Arctic sediments and suggests careful consideration of sediment grain size for a reasonable conversion. Nevertheless, the LIBS technique can be useful for determining sediment provenance in the Chukchi Sea after improving the accuracy of the calibration model and considering an application to Arctic marine geology. Such improvements may provide a better understanding of sedimentary composition and provenance in the Arctic Ocean.

#### Acknowledgments

We thank the captain and crews of the IBRV ARAON for operating sample collections during the 2<sup>nd</sup> Western Arctic cruise in 2011. This study was supported by the Basic Science Research Program through the National Research Foundation of Korea (NRF) funded by Ministry of Education (NRF-2016R1A6A3A11931896), and the NRF funded partly by Ministry of Science and ICT (MSICT) (No. NRF-2016R1A2B3015388, PN17100). S.I.N. is also supported by the Basic Core Technology Development Program for the Oceans and the Polar Regions (NRF-2015M1A5A1037243, PN18090) from the NRF funded by the MSICT.

#### Competing financial interests

The authors declare no competing financial interests.

#### Appendix A. Supplementary data

Supplementary data to this article can be found online at <https://doi.org/10.1016/j.sab.2018.05.002>.

#### References

- [1] J. Rakovský, O. Musset, J. Buoncristiani, V. Bichet, F. Monna, P. Neige, P. Veis, Testing a portable laser-induced breakdown spectroscopy system on geological samples, *Spectrochim. Acta B At. Spectrosc.* 74 (2012) 57–65.
- [2] K.-R. Kim, G. Kim, J.-Y. Kim, K. Park, K.-W. Kim, Kriging interpolation method for laser induced breakdown spectroscopy (LIBS) analysis of Zn in various soils, *J. Anal. At. Spectrom.* 29 (2014) 76–84.
- [3] R.S. Harmon, R.E. Russo, R.R. Hark, Applications of laser-induced breakdown spectroscopy for geochemical and environmental analysis: a comprehensive review, *Spectrochim. Acta B At. Spectrosc.* 87 (2013) 11–26.
- [4] G. Kim, J. Kwak, K.-R. Kim, H. Lee, K.-W. Kim, H. Yang, K. Park, Rapid detection of soils contaminated with heavy metals and oils by laser induced breakdown spectroscopy (LIBS), *J. Hazard. Mater.* 263 (2013) 754–760.
- [5] R. Barbini, F. Colao, V. Latic, R. Fantoni, A. Palucci, M. Angelone, On board LIBS analysis of marine sediments collected during the XVI Italian campaign in Antarctica, *Spectrochim. Acta B At. Spectrosc.* 57 (2002) 1203–1218.
- [6] J.D. Ortiz, L. Polyak, J.M. Grebmeier, D. Darby, D.D. Eberl, S. Naidu, D. Nof, Provenance of Holocene sediment on the Chukchi-Alaskan margin based on combined diffuse spectral reflectance and quantitative X-ray diffraction analysis, *Glob. Planet. Chang.* 68 (2009) 73–84.
- [7] R. Stein, K. Fahl, J. Müller, Proxy reconstruction of Cenozoic Arctic Ocean sea-ice history: from IRD to IP25, *Polarforschung* 82 (2012) 37–71.
- [8] R. Stein, *Arctic Ocean Sediments: Processes, Proxies, and Paleoenvironment*, Elsevier, Amsterdam, 2008.
- [9] M. Yamamoto, S.-I. Nam, L. Polyak, D. Kobayashi, K. Suzuki, T. Irino, K. Shimada, Holocene dynamics in the Bering Strait inflow to the Arctic and the Beaufort Gyre circulation based on sedimentary records from the Chukchi Sea, *Clim. Past* 13 (2017) 1111–1127.
- [10] A. Hu, G.A. Meehl, W. Han, A. Timmermann, B. Otto-Bliesner, Z. Liu, W.M. Washington, W. Large, A. Abe-Ouchi, M. Kimoto, Role of the Bering Strait on the hysteresis of the ocean conveyor belt circulation and glacial climate stability, *Proc. Natl. Acad. Sci.* 109 (2012) 6417–6422.
- [11] S.A. Elias, S.K. Short, H.H. Birks, Late Wisconsin environments of the Bering land bridge, *Palaeogeogr. Palaeoclimatol. Palaeoecol.* 136 (1997) 293–308.
- [12] S.A. Elias, S.K. Short, C.H. Nelson, H.H. Birks, Life and times of the Bering land bridge, *Nature* 382 (1996) 60–63.
- [13] L.D. Keigwin, J.P. Donnelly, M.S. Cook, N.W. Driscoll, J. Brigham-Grette, Rapid sea-level rise and Holocene climate in the Chukchi Sea, *Geology* 34 (2006) 861–864.
- [14] A.-K. Meinhardt, C. März, R. Stein, H.-J. Brumsack, Regional variations in sediment geochemistry on a transect across the Mendeleev Ridge (Arctic Ocean), *Chem. Geol.* 369 (2014) 1–11.
- [15] D. Kobayashi, M. Yamamoto, T. Irino, S.-I. Nam, Y.-H. Park, N. Harada, K. Nagashima, K. Chikita, S.-I. Saitoh, Distribution of detrital minerals and sediment color in western Arctic Ocean and northern Bering Sea sediments: changes in the provenance of western Arctic Ocean sediments since the last glacial period, *Polar Sci.* 10 (2016) 519–531.
- [16] I.W. Croudace, A. Rindby, R.G. Rothwell, ITRAX: description and evaluation of a new multi-function X-ray core scanner, *Geol. Soc. Lond. Spec. Publ.* 267 (2006) 51–63.
- [17] G. Kim, Y.-J. Yoon, H.-A. Kim, H.-j. Cho, K. Park, Elemental composition of Arctic soils and aerosols in Ny-Ålesund measured using laser-induced breakdown spectroscopy, *Spectrochim. Acta B At. Spectrosc.* 134 (2017) 17–24.
- [18] R. Stein, *Accumulation of Organic Carbon in Baffin Bay and Labrador Sea Sediments (ODP-Leg 105)*, Springer, Berlin, 1991.
- [19] D. Han, S.-I. Nam, J.-H. Kim, R. Stein, F. Niessen, Y.J. Joe, Y.-H. Park, H.-G. Hur, Inference on paleoclimate change using microbial habitat preference in Arctic Holocene sediments, *Sci. Rep.* 7 (2017) 9652.
- [20] S.E. MacLachlan, J.E. Hunt, I.W. Croudace, An empirical assessment of variable water content and grain-size on X-ray fluorescence core-scanning measurements of deep sea sediments, *Micro-XRF Studies of Sediment Cores*, Springer, Dordrecht 2015, pp. 173–185.

- [21] M. Jakobsson, R. Løvlie, H. Al-Hanbali, E. Arnold, J. Backman, M. Mörth, Manganese and color cycles in Arctic Ocean sediments constrain Pleistocene chronology, *Geology* 28 (2000) 23–26.
- [22] C. März, A. Stratmann, J. Matthießen, A.-K. Meinhardt, S. Eckert, B. Schnetger, C. Vogt, R. Stein, H.-J. Brumsack, Manganese-rich brown layers in Arctic Ocean sediments: composition, formation mechanisms, and diagenetic overprint, *Geochim. Cosmochim. Acta* 75 (2011) 7668–7687.
- [23] K.D. Daskalakis, T.P. O'connor, Normalization and elemental sediment contamination in the coastal United States, *Environ. Sci. Technol.* 29 (1995) 470–477.
- [24] A.K. Pathak, R. Kumar, V.K. Singh, R. Agrawal, S. Rai, A.K. Rai, Assessment of LIBS for spectrochemical analysis: a review, *Appl. Spectrosc. Rev.* 47 (2012) 14–40.
- [25] D. Hanslik, L. Löwemark, M. Jakobsson, Biogenic and detrital-rich intervals in central Arctic Ocean cores identified using X-ray fluorescence scanning, *Polar Res.* 32 (2013) 18386.
- [26] L. Polyak, J. Bischof, J.D. Ortiz, D.A. Darby, J.E. Channell, C. Xuan, D.S. Kaufman, R. Løvlie, D.A. Schneider, D.D. Eberl, Late Quaternary stratigraphy and sedimentation patterns in the western Arctic Ocean, *Glob. Planet. Chang.* 68 (2009) 5–17.